sdg interacting-boson model in the SU(3) scheme and its application to ^{168}Er

N. Yoshinaga*
Department of Theoretical Physics, Oxford University, 1 Keble Road, Oxford, United Kingdom

Y. Akiyama
Department of Physics, College of Humanities and Sciences, Nihon University, Tokyo 156, Japan

A. Arima
Department of Physics, Faculty of Science, University of Tokyo, Tokyo 113, Japan
(Received 15 October 1987)

The *sdg* interacting-boson model is presented in the SU(3) tensor formalism. The interactions are decomposed according to their SU(3) tensor character. The existence of the SU(3)-seniority preserving operator is found to be important. The model is applied to ^{168}Er. Energy levels and electromagnetic transitions are calculated. This model is shown to solve the problem of anharmonicity regarding the excitation energy of the first $K^\pi=4^+$ band relative to that of the first $K^\pi=2^+$ one. $E4$ transitions are calculated to give different predictions from those by the quasiparticle-phonon nuclear model.

I. INTRODUCTION

The interacting-boson model with s and d bosons (*sd*-IBM) has been successful in describing the low-lying collective states in medium and heavy nuclei. In spite of its wide range of success, it has recently turned out that the model needs other degrees of freedom. One of them is the hexadecapole degree of freedom.[1,2] One evidence for the necessity of this degree of freedom is the systematic appearance of the $K^\pi=3^+$ band in well-deformed nuclei. The excitation energy of this band is generally about 1.5 times that of the γ band. The $K^\pi=3^+$ band is certainly beyond the description of the *sd*-IBM without proton-neutron asymmetry. Another evidence concerns the anharmonic appearance of the $K_i^\pi=4_1^+$ band relative to the γ band in ^{168}Er, which was pointed out by Bohr and Mottelson and other collaborators.[3,4] They criticized the IBM because the *sd*-IBM gives only harmonic solution to the $K_i^\pi=4_1^+$ band.[5,6]

In our recent letter[7] we proposed the *sdg*-interacting boson model[8] (*sdg*-IBM) in order to solve the above problems. It was found that most properties of ^{168}Er including the anharmonic property are well described within this model. Here we present our method of calculating energy and transition matrix elements, which enables one to apply the *sdg*-IBM to other nuclei. The essential results were written in the letter, but detailed discussion is given here. We try to make the paper as self-contained as possible. In addition $E4$ excitations are newly discussed.

In the present paper we show that phenomenologically the problems described above can be solved in one consistent model: the *sdg*-IBM. We diagonalize the *sdg*-IBM Hamiltonian and calculate electromagnetic transitions using one-body operators. In Sec. II our model and method of present calculation are described. In Sec. III the effective interaction is determined in order to reproduce the collective low-lying states of ^{168}Er. It is shown that the total number of free parameters is reduced to six in order to reproduce the anharmonicity. The results are compared with experiment. In Sec. IV a quadrupole operator is defined and calculated $E2$ transition rates are compared with experiment, the geometrical model and the *sd*-IBM. By assuming a one-body magnetic dipole operator, $M1$ transitions are calculated in the *sdg*-IBM, and the results are compared with those of the *sd*-IBM2. $E4$ transitions are also calculated and the excitation strength from the ground state to the $I^\pi=4^+$ of the $K_i^\pi=3_1^+$ band is predicted to be strong. Our model gives different predictions from the quasiparticle-nuclear-phonon model (QPNM).[9] Summary and conclusions are given in Sec. V. From now on, we use abbreviations g, β, and γ for the ground-state band, the next lowest $K^\pi=0^+$ band and the first $K^\pi=2^+$ band, respectively.

II. MODEL AND METHOD OF CALCULATION

The *sd*-IBM has a U(6) dynamical symmetry, while the *sdg*-IBM has a U(15) dynamical symmetry. In this section the U(15) model and our method of calculating energy and transition matrix elements are described. We take the U(15)$\supset$SU(3) scheme among other dynamical symmetries[10] since ^{168}Er is a well deformed nucleus. The number of active bosons, N, is taken to be 16. In Sec. II A all possible one- and two-body interactions are classified according to the U(15)$\supset$SU(3) scheme, which enables us to use the U(15)$\supset$SU(3) Racah algebra. Explicit formulae for calculating energies and transition matrix elements are given in Sec. II B. Because a totally symmetric rep (where rep stands for representation) $[N]$ in the U(15) model has a large number of SU(3) reps for $N=16$, we are obliged to truncate our model space. The way we choose the truncated basis states, which are in-

cluded in our calculation, is described in Sec. II C. The SU(3) algebra used in this calculation was given by Draayer and Akiyama.[11]

A. Interactions in the U(15)⊃SU(3) scheme

In the U(15) model the one-boson state belongs to the (40) rep in the SU(3) notation (λ,μ), while it belongs to the (20) rep in the U(6) model. Two-boson states (which must be symmetric) are classified by three reps (80), (42), and (04) in the U(15) model, while there appear only two reps (40) and (02) in the U(6) model.

In the U(15) model the creation and annihilation operators $b^\dagger_{lm}$ and $\tilde{b}_{lm}$ for bosons transform as (40) and (04) reps of the SU(3) group, respectively, where $\tilde{b}_{lm}\equiv(-)^{l+m}b_{l-m}$ and $l=0,2,4$.

In the boson rep any one-body operator with angular momentum L is written as

$$T_1^{\lambda KLM}=\Sigma((40)l_1m_1(04)l_2m_2\,|\,(\lambda,\lambda)KLM)\times b^\dagger_{l_1m_1}\tilde{b}_{l_2m_2}\quad(\lambda=0,1,2,3,4)\,. \tag{2.1}$$

Here $((40)lm(04)l'm'\,|\,(\lambda,\mu)KLM)$ are the Clebsch-Gordon coefficients of the SU(3) group. In particular, $T^{\lambda=1}$ are the generators of SU(3). In this paper it is assumed that the electromagnetic operator is written as a one-body boson operator. Thus, it can be expressed as

$$Q^L_M=\Sigma\alpha_{\lambda K}T_1^{\lambda KLM}\,, \tag{2.2}$$

where $\alpha_{\lambda K}$'s are constants to be determined.

Next we construct the two-body scalar interaction which has a definite U(15)⊃SU(3) tensor character. We define two-particle boson and two-hole boson operators as follows:

$$B^\dagger(\lambda,\mu)^{KLM}\equiv[b^\dagger b^\dagger]^{(\lambda,\mu)KLM}\equiv\Sigma((40)lm(40)l'm'\,|\,(\lambda,\mu)KLM)b^\dagger_{lm}b^\dagger_{l'm'},\quad(\lambda,\mu)=(8,0),(4,2),(0,4) \tag{2.3a}$$

and

$$\tilde{B}(\mu,\lambda)^{KLM}\equiv[\tilde{b}\tilde{b}]^{(\mu,\lambda)KLM}\equiv\Sigma((04)lm(04)l'm'\,|\,(\mu,\lambda)KLM)\tilde{b}_{lm}\tilde{b}_{l'm'},\quad(\mu,\lambda)=(0,8),(2,4),(4,0)\,. \tag{2.3b}$$

For energy operators which are written as one- and two-body interactions, we will omit K,L,M (all equal to zero).

Two-body scalar interactions in SU(3) tensor reps defined as

$$[B^\dagger(\lambda,\mu)\tilde{B}(\mu',\lambda')]^{(\lambda_0,\mu_0)\rho}$$

are not yet reduced in U(15). Here ρ distinguishes independent modes of coupling in SU(3). This label is needed only in the coupling (42)×(24). One constructs U(15) tensor operators by the following linear combination:

$$T_2^{[F_0](\lambda_0,\mu_0)A_0}=\Sigma\langle[\bar{2}](\mu',\lambda')[2](\lambda,\mu)\|[F_0](\lambda_0,\mu_0)A_0\rangle_\rho\times[B^\dagger(\lambda,\mu)\tilde{B}(\mu',\lambda')]^{(\lambda_0,\mu_0)\rho}\,. \tag{2.4}$$

The A_0 represents the additional label which uniquely specifies the U(15)⊃SU(3) reduction. The overbar on the label [2] shows that it is a hole rep. We have three different labels for the U(15) label $[F_0]$; [0], $[21^{13}]$, and $[42^{13}]$. Interactions in terms of the U(15)⊃SU(3) scheme are shown in Table I. In the U(6) model we have two one-body and seven two-body scalar interactions which are Hermitian.[12] In the U(15) model we have three one-body and 32 two-body scalar interactions which are Hermitian. The number of two-body interactions increases up to 48 if antihermitian operators are allowed. This extension of interactions is necessary when one derives boson-interactions microscopically using the Dyson boson mapping. All U(15)⊃SU(3) reduction coefficients are listed in Table II.

B. Method of calculation

Any ν-body interaction is decomposed according to the U(15)⊃SU(3)⊃O(3) scheme as

$$V^{L_0}=\Sigma V^{[F_0](\Lambda_0M_0)A_0K_0L_0}\,, \tag{2.5}$$

where $[F_0]$, (Λ_0M_0), and L_0 are the reps of U(15), SU(3), and O(3), respectively. The O(3) is nothing but the physical rotational group. The totally symmetric state according to the U(15)⊃SU(3)⊃O(3) scheme is represented as

$$|\,[N](\Lambda M)AKL\,\rangle\,,$$

where (ΛM) is the rep of SU(3) and A is the additional label which uniquely specifies the U(15)⊃SU(3) reduction. The direct product of the totally symmetric $(N-1)$-body and one-body states

$$|\,[N-1](\Lambda M)AKL\,\rangle\,|\,[1](40)kl\,\rangle$$

is not totally symmetric. In the next subsection we discuss how to obtain the totally symmetric states using the Majorana operator.

The reduced matrix element of a ν-body ($\nu\leq2$) force is for an N-body totally symmetric system

TABLE I. Interaction tensor operators for bosons in the *sdg*-IBM.

$[F_0]$	SU(3) labels	One-body	Two-body Hermite	Two-body Anti-Hermite
[0]	(0,0)	1	1	
$[21^{13}]$	(2,2)	1	1	
	(4,4)	1	1	
$[42^{13}]$	(0,0)		2	
	(2,2)		6	2
	(6,0),(0.6)		4	4
	(4,4)		7	3
	(6,6)		3	1
	(8,2),(2,8)		4	4
	(12,0),(0,12)		1	1
	(10,4),(4,10)		1	1
	(8,8)		1	
Total		3	32	16

$$\langle [N](\Lambda_1 M_1) A_1 K_1 L_1 \| V^{L_0} \| [N](\Lambda_2 M_2) A_2 K_2 L_2 \rangle$$
$$= \sqrt{2L_1+1} \begin{bmatrix} N \\ \nu \end{bmatrix} \Sigma (-)^{\kappa} \sqrt{dim(\Lambda_2 M_2)/dim(\Lambda M)} ([\nu] \| \| V^{[F_0](\Lambda_0 M_0) A_0 K_0 L_0} \| \| [\bar{\nu}])$$
$$\times U((\Lambda_2 M_2)(\mu_2 \lambda_2)(\Lambda_1 M_1)(\lambda_1 \mu_1); (\Lambda M)(\Lambda_0 M_0))_{\rho_2 \rho_1 \rho_3 \rho}$$
$$\times \langle [N-\nu](\Lambda M) A [\nu](\lambda_1 \mu_1) \| [N](\Lambda_1 M_1) A_1 \rangle_{\rho_1} \langle [N-\nu](\Lambda M) A [\nu](\lambda_2 \mu_2) \| [N](\Lambda_2 M_2) A_2 \rangle_{\rho_3}$$
$$\times \langle [\bar{\nu}](\mu_2 \lambda_2)[\nu](\lambda_1 \mu_1) \| [F_0](\Lambda_0 M_0) A_0 \rangle_{\rho_2} \langle (\Lambda_2 M_2) K_2 L_2 (\Lambda_0 M_0) K_0 L_0 \| (\Lambda_1 M_1) K_1 L_1 \rangle_{\rho} \quad (2.6)$$

and

$$\kappa = \Lambda_2 + M_2 + \lambda_2 + \mu_2 + \Lambda + M \ .$$

The quantum number ρ distinguishes independent modes of coupling in SU(3).

In Eq. (2.6) the SU(3) Racah-coefficient U is defined in Ref. 13. The first factors

$$\langle [N-\nu](\Lambda M) A [\nu](\lambda_1 \mu_1) \| [N](\Lambda_1 M_1) A_1 \rangle_{\rho_1}$$

are the coefficients of fractional parentage (cfp) which are obtained by the method described in the next subsection. The second factors

$$\langle [\bar{\nu}](\mu_2 \lambda_2)[\nu](\lambda_1 \mu_1) \| [F_0](\Lambda_0 M_0) A_0 \rangle_{\rho_2}$$

are the same isoscalar U(15)$\supset$SU(3) coefficients as appeared in Eq. (2.4) for two-body interactions ($\nu=2$) and are unity for one-body interactions ($\nu=1$). The third factors

$$\langle (\Lambda_2 M_2) K_2 L_2 (\Lambda_0 M_0) K_0 L_0 \| (\Lambda_1 M_1) K_1 L \rangle_{\rho}$$

are the SU(3)-isoscalar factors.[13]

The triple-barred matrix element in Eq. (2.6) can be derived from the given boson interaction

$$([\nu](\lambda_1 \mu_1) k_1 l_1 \mid V \mid [\nu](\lambda_2 \mu_2) k_2 l_2)$$

by using the following formula:

$$([\nu] \| \| V^{[F_0](\Lambda_0 M_0) A_0 K_0 L_0} \| \| [\bar{\nu}]) = \Sigma \langle [\bar{\nu}](\mu_2 \lambda_2)[\nu](\lambda_1 \mu_1) \| [F_0](\Lambda_0 M_0) A_0 \rangle_{\rho} \langle (\mu_2 \lambda_2) \bar{k}_2 l_2 (\lambda_1 \mu_1) k_1 l_1 \| (\Lambda_0 M_0) K_0 L_0 \rangle_{\rho}$$
$$\times ([\nu](\lambda_1 \mu_1) k_1 l_1 \mid V \mid [\nu](\lambda_2 \mu_2) k_2 l_2) \ . \quad (2.7)$$

TABLE II. The complete reduction coefficients $\langle[\bar{2}](\mu',\lambda')[2](\lambda,\mu)\,|\,[F_0](\lambda_0,\mu_0)\rangle_{\rho\sigma}$ for the U(15)⊃SU(3) are listed. The numbers [ ] in the first column of this table show the shorthand notations of the U(15) reps, i.e., $[1]=[0],[2]=[21^{13}],[3]=[42^{13}]$ representing $[F_0]$. For example, $\langle[\bar{2}](40)[2](42)\|[42^{13}](22)\rangle_{\sigma=3}=0.481\,879$. We need multiplicity label ρ only for the coupling (24)×(42). In the text σ is denoted as A_0.

(μ',λ')		(08)				(24)				(40)	
(λ,μ)	(80)	(42)	(04)	(80)	(42)	(42)	(42)	(04)	(80)	(42)	(04)
$[F_0](\lambda_0,\mu_0)\sigma$					$\rho=1$	$\rho=2$	$\rho=3$				
[1](0 0)1	0.612 372	0.0	0.0	0.0	0.707 107	0.0	0.0	0.0	0.0	0.0	0.353 553
[2](2 2)1	0.597 112	0.268 382	0.0	0.268 382	0.384 025	0.091 073	−0.236 745	0.361 551	0.0	0.361 551	0.161 690
[2](4 4)1	0.219 242	0.471 008	0.291 043	0.471 008	0.054 924	0.248 243	0.413 102	0.216 930	0.291 043	0.216 930	0.097 014
[3](0 0)1	0.765 532	0.0	0.0	0.0	−0.418 718	0.0	0.0	0.0	0.0	0.0	−0.488 504
[3](0 0)2	0.197 386	0.0	0.0	0.0	−0.569 803	0.0	0.0	0.0	0.0	0.0	0.797 724
[3](2 2)1	0.607 595	−0.251 070	0.0	−0.251 070	0.287 542	−0.301 185	0.316 050	−0.338 229	0.0	−0.338 229	0.051 747
[3](2 2)2	0.119 873	−0.049 534	0.0	−0.049 534	0.056 729	−0.059 421	0.062 354	0.150 581	0.0	0.150 581	−0.961 632
[3](2 2)3	−0.058 999	−0.362 111	0.0	−0.362 111	−0.104 035	−0.261 164	0.379 978	0.481 879	0.0	0.481 879	0.215 503
[3](2 2)4	0.0	0.0	0.0	0.0	0.176 832	0.787 859	0.589 922	0.0	0.0	0.0	0.0
[3](2 2)5	0.506 394	−0.045 679	0.0	−0.045 679	−0.823 377	0.237 625	−0.070 545	0.0	0.0	0.0	0.0
[3](2 2)6	0.0	−0.478 822	0.0	−0.478 822	0.215 833	0.389 958	−0.585 498	0.0	0.0	0.0	0.0
[3](2 2)7	0.0	0.707 107	0.0	−0.707 107	0.0	0.0	0.0	0.0	0.0	0.0	0.0
[3](2 2)8	0.0	0.0	0.0	0.0	0.0	0.0	0.0	0.707 107	0.0	−0.707 107	0.0
[3](4 4)1	0.0	0.295 804	0.0	0.295 804	0.0	0.0	0.0	−0.642 262	0.0	−0.642 262	0.0
[3](4 4)2	0.0	−0.314 343	0.616 626	−0.314 343	0.0	0.0	0.0	−0.144 776	0.616 626	−0.144 776	0.0
[3](4 4)3	0.975 670	−0.105 840	−0.065 400	−0.105 840	−0.012 342	−0.055 783	−0.092 828	−0.048 746	−0.065 400	−0.048 746	−0.021 800
[3](4 4)4	0.0	−0.027 219	−0.016 819	−0.027 219	0.998 414	−0.014 346	−0.023 873	−0.012 536	−0.016 819	−0.012 536	−0.005 606
[3](4 4)5	0.0	−0.127 426	−0.078 738	−0.127 426	0.0	0.966 984	−0.111 760	−0.058 688	−0.078 738	−0.058 688	−0.026 246
[3](4 4)6	0.0	−0.244 007	−0.150 775	−0.244 007	0.0	0.0	0.898 705	−0.112 381	−0.150 775	−0.112 381	−0.050 258
[3](4 4)7	0.0	−0.064 185	−0.039 661	−0.064 185	0.0	0.0	0.0	−0.029 562	−0.039 661	−0.029 562	0.993 412
[3](4 4)8	0.0	0.707 107	0.0	−0.707 107	0.0	0.0	0.0	0.0	0.0	0.0	0.0
[3](4 4)9	0.0	0.0	0.707 107	0.0	0.0	0.0	0.0	0.0	−0.707 107	0.0	0.0
[3](4 4)10	0.0	0.0	0.0	0.0	0.0	0.0	0.0	0.707 107	0.0	−0.707 107	0.0
[3](6 0)1	0.0	0.0	0.0	1.000 000	0.0	0.0	0.0	0.0	0.0	0.0	0.0
[3](6 0)2	0.0	0.0	0.0	0.0	1.000 000	0.0	0.0	0.0	0.0	0.0	0.0
[3](6 0)3	0.0	0.0	0.0	0.0	0.0	0.0	0.0	1.000 000	0.0	0.0	0.0
[3](6 0)4	0.0	0.0	0.0	0.0	0.0	0.0	0.0	0.0	0.0	1.000 000	0.0
[3](0 6)1	0.0	1.000 000	0.0	0.0	0.0	0.0	0.0	0.0	0.0	0.0	0.0
[3](0 6)2	0.0	0.0	0.0	0.0	1.000 000	0.0	0.0	0.0	0.0	0.0	0.0
[3](0 6)3	0.0	0.0	0.0	0.0	0.0	0.0	0.0	0.0	0.0	1.000 000	0.0
[3](0 6)4	0.0	0.0	0.0	0.0	0.0	0.0	0.0	1.000 000	0.0	0.0	0.0
[3](6 6)1	1.000 000	0.0	0.0	0.0	0.0	0.0	0.0	0.0	0.0	0.0	0.0
[3](6 6)2	0.0	0.0	0.0	0.0	1.000 000	0.0	0.0	0.0	0.0	0.0	0.0
[3](6 6)3	0.0	0.707 107	0.0	0.707 107	0.0	0.0	0.0	0.0	0.0	0.0	0.0
[3](6 6)4	0.0	0.707 107	0.0	−0.707 107	0.0	0.0	0.0	0.0	0.0	0.0	0.0
[3](8 8)1	1.000 000	0.0	0.0	0.0	0.0	0.0	0.0	0.0	0.0	0.0	0.0
[3](8 2)1	0.0	0.0	0.0	1.000 000	0.0	0.0	0.0	0.0	0.0	0.0	0.0

TABLE II. (*Continued*).

(μ',λ') (λ,μ) $[F_0](\lambda_0,\mu_0)\sigma$	(80)	(08) (42)	(04)	(80)	(42) $\rho=1$	(24) (42) $\rho=2$	(42) $\rho=3$	(04)	(80)	(40) (42)	(04)
[3](8 2)2	0.0	0.0	0.0	0.0	1.000 000	0.0	0.0	0.0	0.0	0.0	0.0
[3](8 2)3	0.0	0.0	0.0	0.0	0.0	0.0	0.0	0.0	1.000 000	0.0	0.0
[3](8 2)4	0.0	0.0	0.0	0.0	0.0	0.0	0.0	0.0	0.0	1.000 000	0.0
[3](2 8)1	0.0	1.000 000	0.0	0.0	0.0	0.0	0.0	0.0	0.0	0.0	0.0
[3](2 8)2	0.0	0.0	0.0	0.0	1.000 000	0.0	0.0	0.0	0.0	0.0	0.0
[3](2 8)3	0.0	0.0	1.000 000	0.0	0.0	0.0	0.0	0.0	0.0	0.0	0.0
[3](2 8)4	0.0	0.0	0.0	0.0	0.0	0.0	0.0	1.000 000	0.0	0.0	0.0
[3](12 0)1	0.0	0.0	0.0	0.0	0.0	0.0	0.0	0.0	1.000 000	0.0	0.0
[3](0 12)1	0.0	0.0	1.000 000	0.0	0.0	0.0	0.0	0.0	0.0	0.0	0.0
[3](10 4)1	0.0	0.0	0.0	1.000 000	0.0	0.0	0.0	0.0	0.0	0.0	0.0
[3](4 10)1	0.0	1.000 000	0.0	0.0	0.0	0.0	0.0	0.0	0.0	0.0	0.0

C. Basis states and truncation

We find SU(3) reps belonging to $[N]$ by diagonalizing the Majorana operator among the basis states with the same SU(3) label. This procedure simultaneously provides us with coefficients of fractional parentage (cfp):

$$\langle [N-\nu](\Lambda M)A[\nu](\lambda\mu)\|[N](\Lambda' M')A'\rangle_\rho \ .$$

Table III shows the thus obtained totally symmetric states appearing in the *sdg*-IBM for $N=1,2,3,4,5$. When $N=4$, the (8,4) rep appears twice. A general method, which distinguishes states with the same (λ,μ) reps satisfying $\lambda+2\mu=4N$ in a more physical way than those obtained by the simple diagonalization of the Majorana operator, is established in Ref. 12. The distinction between these two reps with $\mu=4$ according to this description turns out to give an important clue to understanding the properties of the $K_i^\pi=4_1^+$ band in well deformed nuclei.

In order to obtain the cfp's for the states satisfying the restriction $\lambda+2\mu=4N$ for the N-body system following this procedure, we diagonalize an operator defined by

$$S=[B^\dagger(04)\tilde{B}(40)]^{(00)} \ . \tag{2.8}$$

according to the SU(3)-seniority classification within the fully symmetric states $[N]$. The resulting basis states are characterized by the SU(3)-seniority quantum number w, where w means the number of boson pairs coupled to (04) rep in Ref. 12. In terms of w the eigenvalue of the S operator is

$$(375)^{-1/2}w(2N-2w+3) \tag{2.9}$$

for the states with $\lambda+2\mu=4N$.

In the other cases of (λ,μ) with $\lambda+2\mu<4N$ we may still use the same procedure; the S operator is diagonalized within the fully symmetric boson states. However, the eigenvalues of the S operator, in general, cannot be expressed as simply as the formula (2.9). There are, however, certain states which have zero eigenvalue. These states can be labeled with $w=0$.

In order to see the effect of the S operator we diagonalize the Hamiltonian which includes the S operator in addition to the Casimir operator and L^2 operator. The result is presented in Fig. 1. The bands with $w=0$ stay at their SU(3) limit positions. The $w=1$ bands are located at different positions from their SU(3) limits. For example, compare the location of (56,4) $w=0$, $K=0$ with that of (56,4) $w=1$, $K=0$. The former energy is 3.148 MeV which coincides with an eigenvalue of the Casimir operator. In analogy to Eq. (2.8) two more operators

$$U=[B^\dagger(04)\tilde{B}(40)]^{(22)} \tag{2.10}$$

and

$$Z=[B^\dagger(04)\tilde{B}(40)]^{(44)} \tag{2.11}$$

are introduced. These operators have the interesting and important property that they do not have any effect on the states with $w=0$ including states with $\lambda+2\mu=4N$ and $\lambda+2\mu<4N$. This is clear by their definitions. Namely they destroy a (04) pair which is not included at

TABLE III. Complete SU(3) representations in the totally symmetric states from [1] to [5] in the U(15) model. The superscript indicates the multiplicity of the irreducible representation.

[1]	(4,0)									
[2]	(8,0)	(4,2)	(0,4)							
[3]	(12,0)		(8,2)	(6,3)	(4,4)		(0,6)			
				(3,3)						
	(6,0)		(2,2)							
	(0,0)									
[4]	(16,0)		(12,2)	(10,3)	$(8,4)^2$		$(4,6)^2$	(0,8)		
				(7,3)	(5,4)	(3,5)				
	(10,0)	(8,1)	$(6,2)^2$	(4,3)	$(2,4)^2$					
		(5,1)		(1,3)						
	$(4,0)^2$		(0,2)							
[5]	(20,0)		(16,2)	(14,3)	$(12,4)^2$	(10,5)	$(8,6)^2$	(6,7)	$(4,8)^2$	(0,10)
				(11,3)	(9,4)	$(7,5)^2$	(5,6)	(3,7)	(1,8)	
	(14,0)	(12,1)	$(10,2)^3$	$(8,3)^2$	$(6,4)^4$	$(4,5)^2$	$(2,6)^3$			
		$(9,1)^2$	(7,2)	$(5,3)^3$	$(3,4)^2$	(1,5)	(2,6)			
	$(8,0)^3$	(6,1)	$(4,2)^4$	(2,3)	$(0,4)^2$					
		(3,1)								
	$(2,0)^2$									

all in any state with $w=0$. By adding them to an SU(3)-preserving Hamiltonian, bands with $w=0$ remain unchanged in their SU(3)-limit positions.

SU(3) reps (λ,μ) in the *sdg*-IBM are classified by a label r, which is defined by $\lambda+2\mu=4N-3r$, where $r=0,1,2,\ldots,[4N/3]$. Most of the low-lying bands are expected to be described in terms of states with $r=0$, because their expectation values of the Casimir operator of SU(3) are large. In analyzing the nucleus for the $N=16$ system, r varies from 0 to 2. Among them further restrictions are made; in the cases of $r=0$, 1, and 2, $\mu\leq 8$, 7, and 6 are taken, respectively. The basis states thus chosen, which are used in this analysis for the $N=16$ system, are summarized in Table IV. One of the (56,4) reps has the quantum number $w=1$ and is denoted by $(56,4)^{w=1}$, the other one with $w=0$ by $(56,4)^{w=0}$ from now on. A recent group theoretical analysis revealed[14] that the $w=1$ member of (56,4) has one-phonon structure and the $w=0$ member has two-phonon structure.

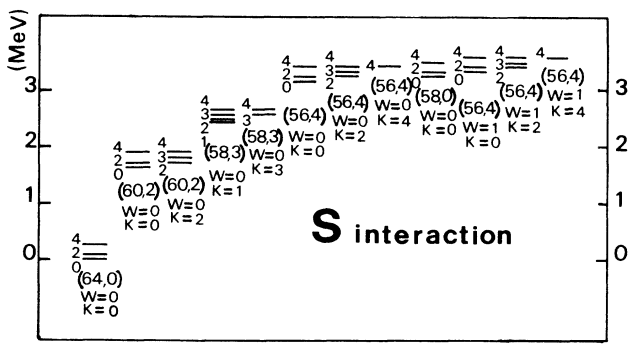

FIG. 1. Energy levels obtained by the SU(3) limit Hamiltonian with an appropriate strength of the S interaction in the *sdg*-IBM.

The problem of truncation of basis states is connected with the nature of the effective interaction. Restricting SU(3) tensor operators to (00), (22), and (60) + (06) tensor operators, as will be done in the following sections, we include in our model space those states which are directly connected by the above interactions with states of $(\lambda,\mu)=(4N,0)$, $(4N-4,2)$, $(4N-6,3)$, and $(4N-8,4)$.

III. ENERGIES

As seen in Sec. II, the number of interactions is so large compared to the *sd* model that we cannot but use only selected interactions which will be later defined. The ^{168}Er nucleus is deformed and exhibits typical rotational band structures. Thus a model Hamiltonian should not destroy the rotational band structure significantly. Higher tensor operators such as the (88) tensor are inadequate in this respect. For simplicity we assume that the Hamiltonian can be expressed by the SU(3) tensor operators (00), (22), and (06) + (60). There are 2, 7, and 4 tensor operators (altogether 13), respectively, for parametrizing the Hamiltonian (see Table I). Among them, the Casimir operator of SU(3), the $\hat{L}^2$ force and the S interaction preserve the SU(3) symmetry. There still remain 10 independent ones, which can be used to describe deviations of energies from the SU(3) limit.

Our procedure for reducing the interaction parameters consists in searching for a few specific interactions, each of which produces some specific effect on the low-lying band positions. The Hamiltonian is parametrized by a combination of them. The most important point in our calculation is the reproduction of the anharmonicity. Thus, in the first place an operator which reproduces this effect should be constructed. Although such an operator

TABLE IV. SU(3) representations used in our present calculation for the $N=16$ system. The states with multiplicity are classified according to the quantum numbers w and δ for the label $r=0$. The δ represents the number of boson-triplets coupled to (06) rep.

$[r]$	(λ,μ)								
[0]	(64,0)		(60,2)	(58,3)	$(56,4)^2$ ($w=0,\delta=0$) ($w=1,\delta=0$)	(54,5)	$(52,6)^3$ ($w=0,\delta=0$) ($w=0,\delta=1$) ($w=1,\delta=0$)	$(50,7)^2$ ($w=0,\delta=0$) ($w=1,\delta=0$)	$(48,8)^4$ ($w=0,\delta=0$) ($w=0,\delta=1$) ($w=1,\delta=0$) ($w=2,\delta=0$)
[1]				(55,3)	(53,4)	$(51,5)^2$	$(49,6)^2$	$(47,7)^3$	
[2]	(58,0)	(56,1)	$(54,2)^3$	$(52,3)^3$	$(50,4)^6$	$(48,5)^6$	$(46,6)^{10}$		

will be found, it will be seen that the operator lowers only $K=2^+$ and $K=4^+$ bands. Therefore we need an operator which lowers $K=0^+$ bands. Finally to adjust the $K_i^\pi=0_3^+$ band, a third operator is constructed.

Because this anharmonic effect is very difficult to obtain,[14] such a requirement imposes a very strong restriction on the selection of the other interactions. As seen in the following we actually have six operators and the same number of free parameters. A detailed procedure for fixing specific operators is explained in Sec. III A. A brief explanation for them is already given in Ref. 15, but a detailed and self-contained description is given there. In Sec. III B the calculated results are compared with experiment.

A. Definition of specific interactions

A Hamiltonian consisting of the Casimir operator $[\langle\hat{C}\rangle=\lambda^2+\mu^2+3(\lambda+\mu)+\lambda\mu]$ and L^2 force $[\langle\hat{L}^2\rangle=L(L+1)]$ with appropriate coefficients is diagonalized and the result is presented in Fig. 2(a). This Hamiltonian is called H_0 hereafter. This figure should be compared to the one in the *sd* model [Fig. 2(b)]. We mention that the energy levels of the SU(3) limit do not satisfy the following requirements; (i) The anharmonicity of the radio, $R=E(K_i^\pi=4_1^+)/E(K_i^\pi=2_2^+)=2.5$ must be reproduced. (ii) The $K_i^\pi=1_1^+$ band must be higher than the $K_i^\pi=4_1^+$ band.

Other SU(3)-breaking interactions must be constructed to meet the above requirements when they are added to the combination of the Casimir operator and the L^2 force. In the earlier calculation[12] one of the authors reported that the anharmonicity could be explained by band mixing between the $w=0$ and $w=1$ members of SU(3) states. This argument was based on a calculation using only $r=0$ states. A further calculation with extended model space as described in the previous section, however, has brought the ratio back to two under the Hamiltonian used in Ref. 12. The failure is attributed to large mixing between $r=0$ and other states of small r. Thus, a further study is needed to find an interaction which reproduces the anharmonicity.

Now the interaction H_1 is constructed as

$$H_1=a[B^\dagger(42)\tilde{B}(08)]^{(06)}+[B^\dagger(80)\tilde{B}(24)]^{(22)}+\text{H.c.}\ , \tag{3.1}$$

where a is determined by requiring

$$\langle(64,0)_{K=0},L=4\,|\,H_1\,|\,(60,2)_{K=0},L=4\rangle=0\ . \tag{3.2}$$

One finds $a=-1.0167$. Thus, the H_1 has a vanishing matrix element between $(64,0)_{K=0}^{L=4}$ (g band) and $(60,2)_{K=0}^{L=4}$ (β band) states. This is necessary because we want to forget about the coupling of g and β for the time being and concentrate ourselves on the coupling between g and γ bands. This turns out to have the effect of satisfying the requirement (i). Figure 3 shows the energy levels obtained by diagonalizing a Hamiltonian obtained by adding the interaction H_1 with an appropriate strength to H_0. One sees in Fig. 3 that the interaction H_1 is particularly useful to reproduce the anharmonic effect. It is seen that we have acquired the ratio $R=2.4$. It should also be

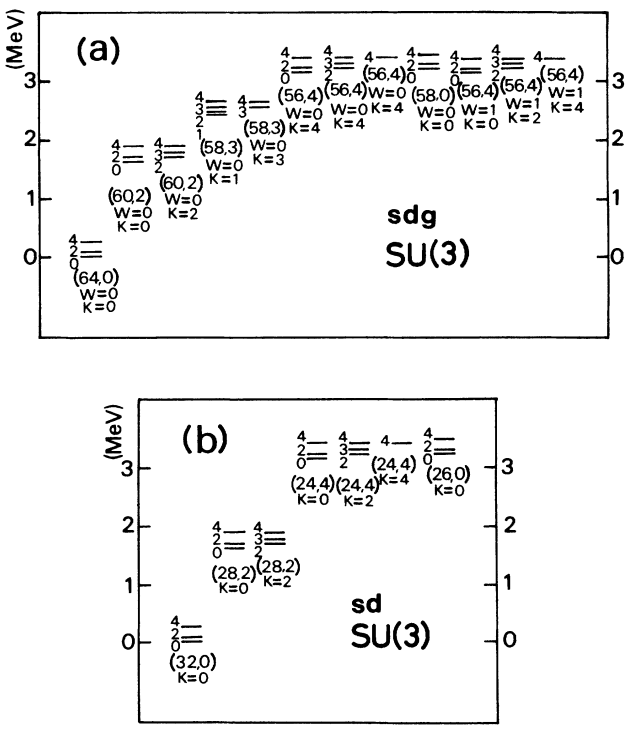

FIG. 2. (a) Similar energy levels as in Fig. 1 without the S interaction. (b) Energy levels in the SU(3) limit in the *sd*-IBM.

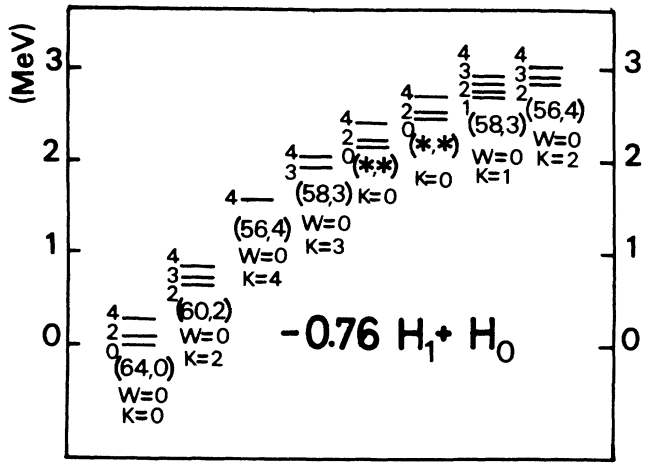

FIG. 3. The Hamiltonian is $-0.76H_1+H_0$, where H_0 is $-0.0043C+0.0013L^2$. The asterisks in the parenthesis $(*,*)$ mean that one cannot assign unique (λ,μ) because the largest amplitude is less than 50%.

noted that the $K^\pi=1^+$ and the $K^\pi=3^+$ bands are already separated in energy from each other by this interaction. Another interesting feature of this Hamiltonian is that all bands except $K^\pi=2^+$ and $K^\pi=4^+$ are pushed up very much. If one is interested only in reproducing the ratio R, and if all bands other than the ground, $K_i^\pi=2_1^+$ and $K_i^\pi=4_1^+$ bands would be found to be not collective, one can be satisfied at this stage. However, we believe that other low-lying bands are also collective. Then we need an interaction which brings down particularly $K^\pi=0^+$ bands in energy. Such an interaction H_2 is constructed as follows.

In the same manner the interaction H_2 is constructed as

$$H_2=b[B^\dagger(42)\tilde{B}(24)]^{(06)}-[B^\dagger(42)\tilde{B}(40)]^{(06)}+\text{H.c.} \tag{3.3}$$

and b is determined by requiring

$$\langle(60,2)_{K=0},L=4\,|\,H_2\,|\,(56,4)^{w=1}_{K=0},L=4\rangle=0\ , \tag{3.4}$$

which gives $b=1.2251$. Figure 4 shows the energy levels obtained by diagonalizing a Hamiltonian obtained by adding the interaction H_2 with an appropriate strength to H_0. The main effect of H_2 is that it lowers the $K_i^\pi=0_2^+$ and $K_i^\pi=0_3^+$ bands. However, the $K_i^\pi=0_3^+$ band is still high in energy.

To lower further the $K_i^\pi=0_3^+$ band, the operator U defined in Eq. (2.10) is found to be useful because it lowers the $(56,4)^{w=1}_{K=0}$ band relative to the $(56,4)^{w=1}_{K=2}$ and $(56,4)^{w=1}_{K=4}$ bands. This operator has no effect on the $w=0$ bands. Figure 5 shows this situation.

The interaction P_1 is introduced in order to shift up or down the $K^\pi=1^+$ band belonging to $(4N-6,3)$ rep without changing the other low-lying states significantly. The operator is constructed in the following way. We have four (22) interactions and three (06) + (60) interactions (altogether seven) which do not admix (8,0) rep with the others (see Table II). Since (64,0) states contain only (8,0) pairs of bosons, these interactions do not connect the (64,0) states with states of other (λ,μ) than (64,0). We expect that the following seven reps are important in addition to the (64,0) rep. They are $(60,2)_{K=0}$, $(60,2)_{K=2}$, $(58.3)_{K=1}$, $(58,3)_{K=3}$, $(56.4)^{w=1}_{K=0}$, $(56,)^{w=1}_{K=2}$, $(56,4)^{w=1}_{K=4}$. There are six off-diagonal matrix elements between a specific state and the other six states. On the other hand one has seven operators. Therefore choosing a specific state, one can construct a linear combination of the operators so that the six nondiagonal matrix elements between the state and the others vanish. We choose the $(58,3)_{K=1}$, as the specific state in order to construct the P_1 interaction. The P_1 interaction is thus constructed to eliminate off-diagonal elements between $(58,3)_{K=1}$ and other six reps in the case of $L=4$. It also has the effect of reducing the SU(3) mixing in the low-lying states. The explicit definition of the P_1 interaction together with those of the H_1, H_2, and U interactions in terms of the U(15)⊃SU(3) irreducible tensor operators is given in Table V. The *sdg*-IBM has the feature that there exist interactions which have an effect only on odd K bands. Figure 6 shows how the $K^\pi=1^+$ band is shifted up by this interaction almost independently of the γ, β,

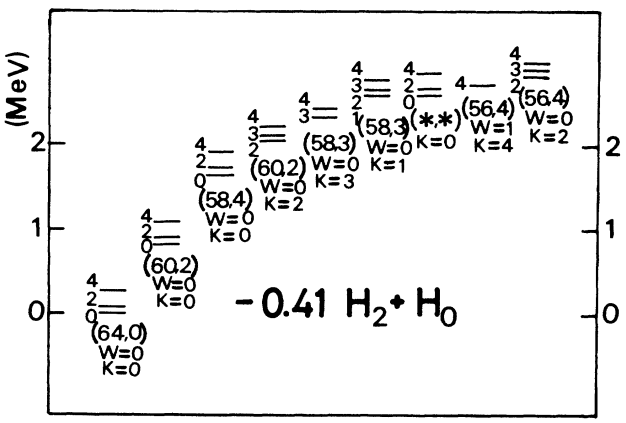

FIG. 4. The Hamiltonian is $-0.41H_2+H_0$.

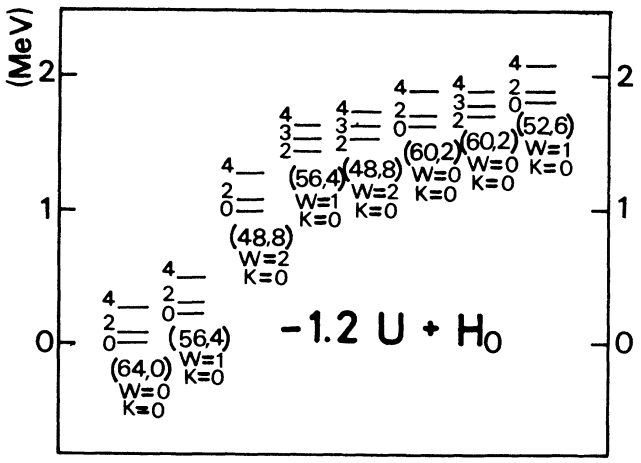

FIG. 5. The Hamiltonian is $-1.2U+H_0$.

TABLE V. Definition of four interactions in Eq. (3.5) except the Casimir operator and L^2 force in terms of the U(15) classified interactions given in Table II. Here $(06)_1$ means $(06)_1+(60)_1$.

$[F_0]$	$[21^{13}]$	$[42^{13}]$								
(λ,μ)	(22)	$(22)_1$	$(22)_2$	$(22)_3$	$(22)_4$	$(22)_5$	$(22)_6$	$(06)_1$	$(06)_2$	$(06)_3$
H_1	0.2684	−0.2511	−0.0495	−0.3621	0.0	−0.0457	−0.4788	1.0167	0.0	0.0
H_2	0.0	0.0	0.0	0.0	0.0	0.0	0.0	0.0	1.2251	−1.0
U	0.1617	0.0517	−0.9616	0.2155	0.0	0.0	0.0	0.0	0.0	0.0
P_1	0.3017	−0.1000	−0.0197	−0.2904	−0.0599	−0.2649	0.4684	0.0	0.0172	0.0

$K^\pi=3^+$, $K^\pi=4^+$, and $w=1$ bands. We will use all these interactions in order to find a phenomenological Hamiltonian which reproduces the level scheme of ^{168}Er.

B. Results

The following Hamiltonian is used for our present calculation:

$$H=a_1H_1+a_2H_2+a_3U+a_4P_1+a_5C_{\mathrm{SU}(3)}+a_6L^2\ , \tag{3.5}$$

where a's are parameters to be determined. The decompositions of the interactions into the U(15)⊃SU(3) tensor operators are listed in Table V.

First we adjust the parameters to the β and γ band excitation energies and the moment of inertia of the g band using the interactions H_1, H_2, $C_{\mathrm{SU}(3)}$, and L^2 (case A in Table VI). The L^2 term is adjusted in order to reproduce the moment of inertia of the g band. The result is shown in Fig. 7. It is seen that the anharmonic feature and the appearance of the $K^\pi=3^+$ band at twice the γ band has been reproduced, but the $K_i^\pi=0_3^+$ band is higher than the $K_i^\pi=4_1^+$ band.

Next, we add the U operator to shift down the $K_i^\pi=0_3^+$ ($w=1$) band (case B in Table VI). The result is shown in Fig. 8. One finds in this figure that the $K_i^\pi=2_3^+$ and $K_i^\pi=0_4^+$ bands also come down. Nevertheless the splitting between $K_i^\pi=0_2^+$ and $K_i^\pi=0_3^+$ is larger than the experimental one because of the large mixing of two SU(3) states, i.e., $(60,2)_{K=0}$ and $(56,4)^{w=1}_{K=0}$.

As stated in Sec. III A the interaction P_1 is useful to reduce the mixing of SU(3) components in $K_i^\pi=0_2^+$ and $K_i^\pi=0_3^+$. Figure 9 shows the energy levels obtained by adding the P_1 operator and adjusting all parameters of the Hamiltonian in Eq. (3.5). A search for the parameters is made in order to reproduce the experimental $K_i^\pi=0_2^+$, $K_i^\pi=2_1^+$, $K_i^\pi=0_3^+$, and $K_i^\pi=4_1^+$ bandhead energies (note $K_i^\pi=0_4^+$, $K_i^\pi=2_2^+$, $K_i^\pi=3_1^+$ bands are not adjusted). The parameters are tabulated in Table VI (case C). The solid lines show the theoretical energy levels and the dashed lines show the bandhead energies of experiment in Fig. 9. Table VII shows the component of bandhead states in terms of SU(3) reps and the expectation values of $\hat{n}_s$, $\hat{n}_d$, and $\hat{n}_g$, i.e., the number operator of s, d, or g bosons. Many bands are strongly admixed. The exceptions are the g, γ, β, and $K_i^\pi=3_1^+$ bands. In the following we discuss the properties of the bands we are interested in. Those bands are excited by some reactions such as the (t,p), (p,t),[16] (d,p), (t,d),[17] (t,α),[18] (α,α'),[19] and (p,p').[20]

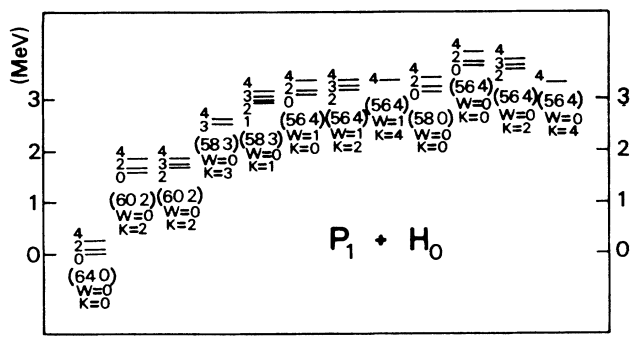

FIG. 6. The Hamiltonian is $1.0P_1+H_0$.

1. *g*, *γ*, *and β bands*

The ground band consists mainly of the (64,0) rep as expected. Among six interactions of the Hamiltonian (3.5) only H_1 mixes (64,0) rep with other reps. The g, β, and γ bands are almost pure SU(3) states. They are $(64,0)_{K=0}$, $(60,2)_{K=0}$, and $(60,2)_{K=2}$ reps, respectively. These bands correspond to $(32,0)_{K=0}$, $(28,2)_{K=0}$, and $(28,2)_{K=2}$ in the sd-IBM.

2. $K_i^\pi=0_3^+$ *band*

This band consists mainly of the $(56,4)^{w=1}$ SU(3) rep. (the overlap is 0.73). This $(56,4)^{w=1}$ state has no counterpart in the sd-IBM. The predicted $K_i^\pi=0_3^+$ band has theoretically the nature of one-phonon state, which is consistent with the recent ^{167}Er(d,p) and ^{167}Er(t,d) experiments. Without this interpretation it seems to be difficult to reproduce the (t,p) strength.[16]

3. $K_i^\pi=0_4^+$ *band*

The fourth $K^\pi=0^+$ band is reproduced at a reasonable position although the energy of this band was not used for our energy fit parametrization. This band consists mainly of the $(52,6)^{w=1}$ rep, but has a small component of the (64,0) rep. In the SU(3) limit this band has no (t,p) strength because of the SU(3) selection rule. This small component of the (64,0) rep, however, makes possible the (t,p) population of this band.[21] In Table II of Ref. 21 relative (t,p) strengths for 0^+ states are predicted by the

TABLE VI. Parameters determined in the boson Hamiltonian in Eq. (3.5). The energy unit is MeV.

Case	a_1	a_2	a_3	a_4	a_5	a_6
A	−0.63	0.31	0.0	0.0	−0.0036	0.013
B	−0.86	0.41	−1.1	0.0	−0.0043	0.013
C	−0.76	0.41	−1.2	1.0	−0.0043	0.013
D	−0.81	0.41	−1.15	0.5	−0.0043	0.013

wave functions obtained by diagonalizing the Hamiltonian in Eq. (3.5).

4. $K_i^\pi=2_2^+$ band

This band is a mixture of the $(56,4)^{w=0}$ and $(56,4)^{w=1}$ reps. (0.63:0.53), i.e., the mixture of one- and two-phonon states. Although the energy of this band was not used for our energy-fit parametrization, its position is well reproduced as seen in Fig. 9. The (t,p) strength predicted for the $I=2$ state of this band is nine times smaller than what is expected for the pure $(56,4)^{w=1}$ state, although it is still four times stronger than that for the pure $w=0$ state. The band mixing causes the reduction of the amplitude for the $w=1$ state and the interference effect. Although the spectroscopic factor is not yet deduced from the experiment, a larger amplitude of the $w=1$ state seems necessary to reconcile the prediction with the experimental observation[16] of a strong (t,p) strength for this state.

5. $K_i^\pi=4_1^+$ band

This band has a large component of $(56,4)^{w=0}$ rep. (0.72). This band corresponds to (24,4) in the *sd*-IBM and has the nature of the 2γ band. The most remarkable feature is the reproduction of the anharmonicity, i.e., $E(K_i^\pi=4_1^+)/E(K_i^\pi=2_1^+)=2.5$, which is mainly due to the effect of configuration mixing. We cannot reproduce this strong anharmonicity using only first order perturbation.

6. $K_i^\pi=3_1^+$ band

We do not use the experimental information on this band. The $K_i^\pi=3_1^+$ band is predicted at a reasonable position. This band is outside the description of the *sd*-IBM1. It has almost pure (58,3) rep, which has one-phonon structure. For quite some time it has been a puzzle whether this band has a collective feature or not. This band is excited by the (t,p) and (α,α') reactions, indicating that this band is collective. In Sec. IV we predict a strong $E4$ excitation of this band. Although the $B(E4)$ is not reported experimentally, the $I=4$ state is definitely populated by the (α,α') reaction.

7. $K^\pi=1^+$ bands

Below 4 MeV we have two $K^\pi=1^+$ bands which are not shown in Fig. 9. One starts at 2.7 MeV and the other at 3.8 MeV. A recent experimental compilation revealed that two $K=1^+$ bands are observed below 2.4 MeV.[22] One starts at 2133 keV, the other at 2365 keV. At this stage we cannot predict which one comes from the hexadecapole degree of freedom. In our model P_1 can shift up and down $K=1^+$ bands without changing the other low-lying states significantly. Thus, adjusting the parameter a_4 in Eq. (3.5) we can fit the theoretical $K=1^+$ band to any of experimental ones. This problem is treated in detail in Sec. IV B.

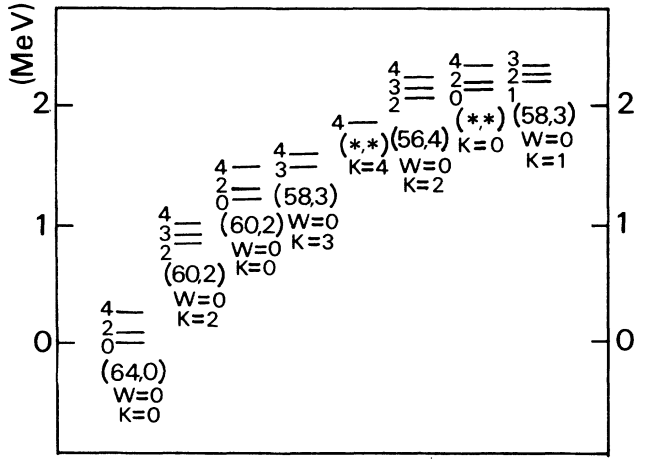

FIG. 7. Only the γ and β bands are fitted in this figure (case *A* in Table VI).

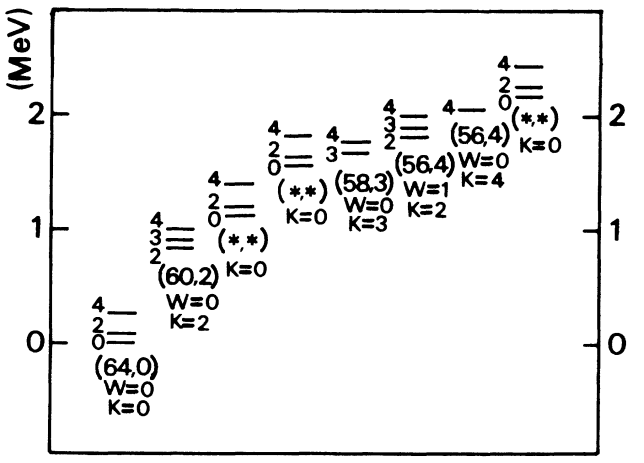

FIG. 8. The γ, β, and $K_i^\pi=0_3^+$ bands are fitted in this figure (case *B* in Table VI).

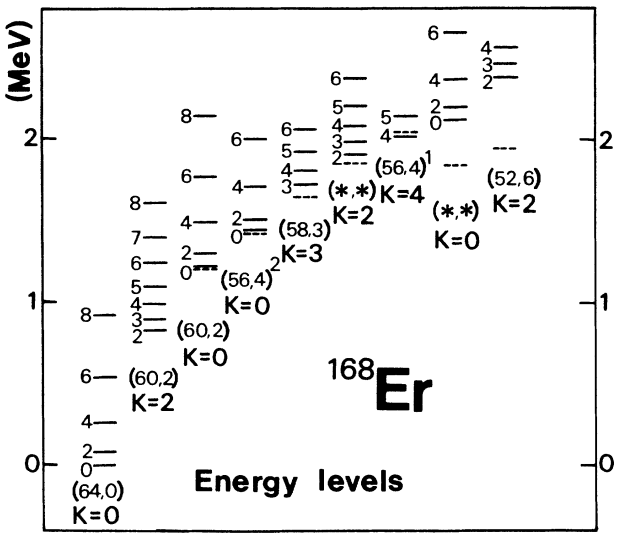

FIG. 9. All parameters appearing in Eq. (3.5) are adjusted in this figure (case *C* in Table VI). Solid lines show calculated energy levels, whereas dashed-lines show experimental bandhead energies.

IV. $E2$, $M1$, AND $E4$ TRANSITIONS

In this section electromagnetic properties are studied within the *sdg*-IBM. The predictions of the geometrical model and the *sd*-IBM are compared with those of the *sdg*-IBM. For that purpose the Mikhailov plot analysis is carried out with respect to $E2$ transitions. One of the differences between the *sdg*-IBM and the *sd*-IBM concerns $M1$ transitions which vanish in the latter without proton-neutron asymmetry. The mechanism of $M1$ transitions is explained in Sec. IV B, where the predictions for $M1$ transitions in ^{168}Er are also given. The theoretical $E4$ operator is determined to reproduce the experimental data taken from an (α,α') experiment.[19]

A. Electric quadrupole transitions

The one-body $E2$ operator is given by four independent parameters in this model:

$$T(E2)=e_1(s^\dagger\tilde{d}+\text{H.c.})+e_2(d^\dagger\tilde{d})^{(2)} +e_3((d^\dagger\tilde{g})^{(2)}+\text{H.c.})+e_4(g^\dagger\tilde{g})^{(2)}\ , \quad (4.1)$$

TABLE VII. The low-lying states obtained by diagonalizing the Hamiltonian in Eq. (3.5) (see case *C* in Table VI). The SU(3) reps are the major ones. The largest component of each state is denoted by asterisk. The subscript distinguishes different states with the same SU(3) rep. The multiplicity was shown in Table IV. The n_b shows the expectation value of *b* bosons.

Bandhead state (MeV)	Representations and their components				n_s	n_d	n_g
g	(64,0)	(58,0)			3.3	9.1	3.7
(0)	0.9047*	0.3962					
2_γ^+	(60,2)	$(56,4)_2$	$(54,2)_2$		3.4	8.8	3.8
(0.8)	0.8308*	−0.3164	−0.3676				
0_2^+	(60,2)	$(56,4)_1$	$(54,2)_2$		3.0	8.5	4.4
(1.2)	0.8092*	0.2940	−0.3473				
0_3^+	$(56,4)_1$	$(56,4)_2$	$(50,4)_2$	$(50,4)_4$	3.4	8.6	4.0
(1.4)	0.4495	0.7282*	−0.2090	0.3002			
2_2^+	$(56,4)_1$	$(56,4)_2$	$(52,6)_3$	$(50,4)_1$	3.0	8.5	4.5
(1.9)	0.6348*	0.5330	−0.2190	0.2183			
3_1^+	(58,3)	$(52,3)_1$			3.0	8.6	4.4
(1.7)	0.9260*	−0.2634					
4_1^+	(58,3)	$(56,4)_1$	$(52,6)_3$	(53,4)	3.3	8.7	4.0
(2.0)	−0.3025	0.7225*	−0.3567	0.2092			
	$(50,4)_1$	$(50,4)_5$					
	0.2448	−0.2080					
0_4^+	(64,0)	$(52,6)_1$	$(52,6)_3$	(58,0)	3.3	8.4	4.3
(2.1)	0.2188	0.3901	0.6929*	−0.2892			
1_1^+	(58,3)	(54,5)	(55,3)	(56,1)	3.1	8.7	4.3
(2.7)	−0.2598	−0.3066	0.5799	0.6111*			
1_2^+	(58,3)	(56,1)	(52,3)		2.9	8.6	4.5
(3.8)	0.7803*	−0.3467	−0.3893				

while in the *sd*-IBM only two independent parameters exist; e_1 and e_2. Equation (4.1) can be transformed into a linear combination of four SU(3) tensor operators defined by Eq. (2.1). In terms of SU(3) tensor operators the *sdg*-IBM has (11), (22), (33), and (44) tensor operators whereas the *sd*-IBM has only (11) and (22) tensors. Explicitly the $E2$ operator is rewritten as

$$T(E2)=\sum_{K\lambda} a_{\lambda K} T_1^{\lambda KL=2} \quad (\lambda=1,2,3,4)\ , \tag{4.2}$$

where $T_1^{\lambda KL\mu}$ is defined in Eq. (2.1). For $(\lambda,\mu)=(22)$ and (44), K takes 0 and 2, but tensor operators with $K=2$ are not independent from those with $K=0$:

$$a_{2,K=2}=\sqrt{21/5}a_{2,K=0},\quad a_{4,K=2}=\sqrt{11/3}a_{4,K=0}\ . \tag{4.3}$$

Therefore we define new Hermitian operators as follows:

$$\hat{T}^{\lambda=2}=\sqrt{5/26}T_i^{\lambda=2,K=0}+\sqrt{21/26}T_1^{\lambda=2,K=2}\ ,$$
$$\hat{T}^{\lambda=4}=\sqrt{3/14}T_1^{\lambda=4,K=0}+\sqrt{11/14}T_1^{\lambda=4,K=2}\ . \tag{4.4}$$

The $E2$ operator is now rewritten in terms of $\hat{T}^{\lambda=2}$ instead of $T^{\lambda=2}$ as

$$T(E2)=\sum_{\lambda}\alpha_\lambda \hat{T}^{\lambda L=2} \quad (\lambda=1,2,3,4)\ . \tag{4.5}$$

The relations between the parameters e's and α's are as follows:

$$\begin{aligned}
\alpha_1&=-\frac{4\sqrt{2}}{5\sqrt{3}}e_1+\frac{11}{7\sqrt{3\times5}}e_2-\frac{36\sqrt{2}}{35\sqrt{3}}e_3+\frac{\sqrt{6\times11}}{7\sqrt{5}}e_4\ ,\\
\alpha_2&=\frac{11}{5\sqrt{3\times7}}e_1-\frac{2\sqrt{2}}{7\sqrt{3\times5\times7}}e_2\\
&\quad+\frac{99}{35\sqrt{3\times7}}e_3+\frac{18\sqrt{11}}{7\sqrt{3\times5\times7}}e_4\ ,\\
\alpha_3&=-\frac{8}{\sqrt{3\times5\times7}}e_1+\frac{11\sqrt{2}}{7\sqrt{3\times7}}e_2\\
&\quad+\frac{68}{7\sqrt{3\times5\times7}}e_3-\frac{\sqrt{11}}{7\sqrt{3\times7}}e_4\ ,\\
\alpha_4&=\frac{\sqrt{11}}{\sqrt{3\times5}}e_1+\frac{2\sqrt{22}}{7\sqrt{3}}e_2-\frac{\sqrt{11}}{7\sqrt{3\times5}}e_3-\frac{2}{7\sqrt{3}}e_4\ .
\end{aligned} \tag{4.6}$$

From experiments two absolute values of $B(E2)$'s are available: $B(E2;0_1^+\rightarrow2_1^+)$ and $B(E2;0_1^+\rightarrow2_2^+)$.[23] For other $B(E2)$'s only relative values are known.

In order to compare our model with the Bohr-Mottelson model we introduce the well-known and well-developed idea in the geometrical model to account for deviations of $E2$ branching ratios from the Alaga rules. Assuming that the intrinsic quadrupole moments do not change from band to band, one can analyze interband $E2$ transitions in terms of the rotational expansion:

$$B(E2;K_iI_i\rightarrow K_fI_f)=(I_iK_i2K_f-K_i\mid I_fK_f)^2[\langle f\mid M_0\mid i\rangle+\langle f\mid M_1\mid i\rangle(I_f(I_f+1)-I_i(I_i+1))]^2 \times\begin{cases}2, & K_i=0\neq K_f \text{ or } K_f=0\neq K_i\\ 1, & \text{otherwise}\ .\end{cases} \tag{4.7}$$

Bohr and Mottelson[3] indeed analyzed the interband $E2$ transitions among the lowest three bands, namely, g, γ, and β. They carried out the Mikhailov plot analyses (MPA) for the $\gamma\rightarrow g$, $\beta\rightarrow g$, and $\beta\rightarrow\gamma$ transitions. The results of their analyses are collected in Table VIII.

We determined the four parameters of $T(E2)$ in (4.5) using the four $\langle f\mid M_0\mid i\rangle$ of their analyses; $g\rightarrow g$, $\gamma\rightarrow g$, $\beta\rightarrow g$, and $\beta\rightarrow\gamma$. For this purpose we have used the wave functions determined by the Hamiltonian given in case C of Table VI. The four determined parameters are $\alpha_1=0.3037$, $\alpha_2=0.0659$, $\alpha_3=-0.0568$, $\alpha_4=-0.1834$. Using the $E2$ operator thus determined, we can calculate any $B(E2)$. However, before discussing our results, we must confirm the consistency of the MPA, whether the assumption used by Bohr and Mottelson holds in our model calculations or not. Table IX shows the calculated intrinsic matrix elements of intraband transitions in the g, γ, and β bands. These elements are found to be almost constant, which confirms the assumption made in the MPA. In the following we compare the calculated results with observed data in each band.

1. g, β, and γ bands

Tables X and XI show the calculated $B(E2)$'s and relative $B(E2)$'s for transitions from the γ and β band states. We list also the prediction by the *sd*-IBM1 made by Warner and Casten.[6] The agreement between theory and experiment for transitions from the γ band is good for each model.

Figure 10 shows the MPA's for $\gamma\rightarrow g$, $\beta\rightarrow\gamma$, and $\beta\rightarrow\gamma$. The general trend of the $E2$ transitions is well

TABLE VIII. $E2$ intrinsic matrix elements. Experimental values and those in the *sd* model are taken from Ref. 3. The case *A* in this table is obtained by the Hamiltonian with the parameters listed as case *C* in Table VI. Similarly the case *B* corresponds to the case *D* in Table VI.

	$E2$ intrinsic matrix elements			
	sd-IBM		Experiment	
	$\langle f\mid M_0\mid i\rangle$	$\langle f\mid M_1\mid i\rangle$	$\langle f\mid M_0\mid i\rangle$	$\langle f\mid M_1\mid i\rangle$
$\gamma\rightarrow g$	25	0.15	28	0.5
$\beta\rightarrow g$	6.5	0.045	4.4	0.06
$\beta\rightarrow\gamma$	19	0.13	12	−0.3
	The present model			
	A		*B*	
	$\langle f\mid M_0\mid i\rangle$	$\langle f\mid M_1\mid i\rangle$	$\langle f\mid M_0\mid i\rangle$	$\langle f\mid M_1\mid i\rangle$
$\gamma\rightarrow g$	29	1.1	30	1.2
$\beta\rightarrow g$	3.8	0.20	5.3	0.06
$\beta\rightarrow\gamma$	11	−0.05	12	−0.45

TABLE IX. Calculated intrinsic matrix elements of intraband transitions in the g, γ, and β bands.

I_i^π	I_f^π	$B(E2)^{1/2}(I020 \mid I0)$
		g intraband
2	0	2.411
4	2	2.413
6	4	2.416
8	6	2.420
		γ intraband
I_i^π	I_f^π	$B(E2)^{1/2}/(I220 \mid I2)$
4	2	2.327
6	4	2.315
8	6	2.296
		β intraband
I_i^π	I_f^π	$B(E2)^{1/2}/(I020 \mid I0)$
2	0	2.262
4	2	2.258
6	4	2.253
8	6	2.246

reproduced, i.e., the theoretical slope of the $\gamma \rightarrow g$, $\beta \rightarrow g$, and $\beta \rightarrow \gamma$ MPA's is positive, positive, and negative, respectively. This is consistent with experiment. It should be remembered that we have adjusted the four parameters to the four $\langle f \mid M_0 \mid i \rangle$'s, but not to $\langle f \mid M_1 \mid i \rangle$'s. Therefore the theoretical $\langle f \mid M_1 \mid i \rangle$'s should be compared with the values derived from the data. The least-squares average M_0's and M_1's are collected in Table VIII (case A). The reproduction for the γ band is a little worse than that by Warner and Casten. Our results, however, reproduce the overall trend of $B(E2)$ transitions.

Since the strength of P_1 interaction was determined rather arbitrarily in Sec. III B, we have changed the parameter a_4 in order to see the effects on MPA's. The strength of P_1 is now reduced to one half of that used in case C (see case D in Table VI). The other interactions are consequently changed a little to reproduce energy levels. The results are summarized in Table VIII as case B. The parameters of the $E2$ operator are then $\alpha_1 = 0.2464$, $\alpha_2 = 0.1245$, $\alpha_3 = 0.1063$, $\alpha_4 = -0.3186$. The $\langle f \mid M_1 \mid i \rangle$'s for $\beta \rightarrow g$ and $\beta \rightarrow \gamma$ are improved. The $\langle f \mid M_1 \mid i \rangle$ of $\gamma \rightarrow g$ is still two times as large as the experimental one. This means that the strength of P_1 affects only the β band.

2. $K_i^\pi = 0_3^+$ band

The $E2$ transitions for $K_i^\pi = 0_3^+ \rightarrow g$ are predicted to be as weak as those for $\beta \rightarrow g$. This fact is also consistent with the experiment.

3. $K_i^\pi = 4_1^+$ band

We find theoretically the following ratio

TABLE X. Comparison of experimental and theoretical $B(E2)$ branching ratios from states of gamma band in ^{168}Er.

Transition		Calculated absolute	Relative $B(E2;I_i \rightarrow I_f)$		
I_i^π	I_f, K	$B(E2;I_i \rightarrow I_f)e^2\text{fm}^2$	*sdg*	IBM1[a]	Expt[a]
2^+	0,0	0.016 41	36.7	66.0	54.0
	2,0	0.044 77	100.0	100.0	100.0
	4,0	0.006 36	14.2	6.0	6.8
3^+	2,0	0.028 39	1.4	2.7	2.6
	4,0	0.041 97	2.1	1.3	1.7
	2,2	1.955 09	100.0	100.0	100.0
4^+	2,0	0.001 86	0.3	2.5	1.6
	4,0	0.052 29	8.1	8.3	8.1
	6,0	0.020 74	3.2	1.0	1.1
	2,2	0.644 65	100.0	100.0	100.0
5^+	4,0	0.012 20	1.2	4.3	2.9
	6,0	0.067 38	6.5	3.1	3.6
	3,2	1.039 06	100.0	100.0	100.0
	4,2	1.050 10	101.0	98.5	122.0
6^+	4,0	0.000 28	0.02	0.97	0.44
	6,0	0.050 53	4.0	4.3	3.8
	8,0	0.036 02	2.9	0.73	1.4
	4,2	1.258 75	100.0	100.0	100.0
	5,2	0.735 18	58.4	59.0	69.0
7^+	6,0	0.003 38	2.4	2.7	0.74
	5,2	1.432 33	100.0	100.0	100.0
	6,2	0.587 42	41.0	39.0	59.0
8^+	6,0	0.005 02	0.34	0.67	1.8
	8,0	0.046 44	3.1	3.5	5.1
	6,2	1.494 68	100.0	100.0	100.0
	7,2	0.403 07	27.0	29.0	135.0

[a]Reference 6.

TABLE XI. Comparison of experimental and theoretical $B(E2)$ branching ratios from states of 0_2^+ band in ^{168}Er.

Transition I_i^π	I_f,K	Calculated absolute $B(E2;I_i\rightarrow I_f)e^2\text{fm}^2$	Relative $B(E2;I_i\rightarrow I_f)$ *sdg*	IBM1[a]	Expt[a]
0^+	2,0	0.004 67	15.9	5.5	5.5
	2,2	0.029 37	100.0	100.0	100.0
2^+	0,0	0.000 26	0.02	0.10	0.23
	2,0	0.000 60	0.05	0.32	1.4
	2,2	0.008 30	0.8	2.6	4.0
	3,2	0.014 47	1.4	4.9	=4.9
	0,0′	1.023 04	100.0	100.0	
4^+	2,0	0.000 14	0.01	0.09	0.02
	6,0	0.007 34	0.50	0.23	0.11
	2,2	0.000 26	0.02	0.04	0.03
	3,2	0.003 03	0.21	0.63	0.35
	4,2	0.009 56	0.65	2.2	0.52
	5,2	0.010 88	0.75	2.8	0.19
	2,0′	1.456 77	100.0	100.0	100.0
6^+	4,0	0.000 06	0.004	0.07	0.02
	8,0	0.017 21	0.70	0.21	0.07
	4,2	0.000 79	0.049	0.09	0.11
	5,2	0.003 45	0.22	0.73	0.32
	6,2	0.009 32	0.59	2.0	0.93
	4,0′	1.596 72	100.0	100.0	100.0

[a]Reference 6.

$$B(E2;K_i^\pi=4_1^+\rightarrow K_i^\pi=2_1^+)/B(E2;K_i^\pi=2_1^+\rightarrow K_i^\pi=0_1^+)\approx 1.4\ .$$

This indicates that the $K_i^\pi=4_1^+$ band has the nature of 2γ band. The states of this band are predicted to decay into mainly the members of the γ band and the $K^\pi=3^+$ band.

B. Magnetic dipole transitions

In the *sd*-IBM one must either introduce a two-body interaction or expand the model to the IBM2 in order that $M1$ transitions occur.[24] On the other hand $M1$ transitions are possible by a one-body operator in the *sdg*-IBM.

The one-body $M1$ operator is given by two independent parameters in this model

$$T(M1)=\sqrt{3/4\pi}(g_d\sqrt{10}(d^\dagger\tilde{d})^{(1)}+g_g\sqrt{60}(g^\dagger\tilde{g})^{(1)})\ . \tag{4.8}$$

The $T(M1)$ with

$$g_d=g_g=(4\pi/3)^{1/2}$$

is nothing but the angular momentum generator. To have finite $M1$ transitions $g_d\neq g_g$ is necessary. The *sdg*-IBM has (11) and (33) SU(3) tensor operators for a one-body operator with angular momentum one. Since the (11) tensor is proportional to the angular momentum operator, only the (33) tensor makes $M1$ transitions occur.

As discussed in Sec. III B up to now we cannot determine which one among two experimentally observed $K^\pi=1^+$ bands[22] corresponds to the $K^\pi=1^+$ band belonging to the (58,3) rep. For the time being, therefore, it is possible to assign the theoretical 1_2^+ state to the 1^+ state at 3.39 MeV found by (e,e') experiment,[25] although the theoretical state is higher in energy compared with experiment. The wave function of the 1^+ state at 3.8 MeV consists mainly of the (58,3) rep whereas the one at 2.7 MeV is mainly a mixture of (55,3) and (56,1) (see Table VII). In order to determine the two g factors appearing in Eq. (4.8), we have taken two experimental values; one is the g factor of the 2_1^+ state ($=0.315[\mu_N]$), and the other $B(M1;0_1^+\rightarrow 1_2^+)_{\text{exp}}(=0.9[\mu_N^2])$. Then we have $g_d=0.548$ and $g_g=0.128$. With this $M1$ operator the g factor of the 4_1^+ state is 0.313, whereas the experimental one is 0.303.[26] In the same way we calculated low-lying $M1$ transitions such as $\gamma\rightarrow g$ transitions using the $M1$ operator. We confirmed that $M1$ transitions among low-lying states are extremely small ($\leq 10^{-3}[\mu_N^2]$), which is within the theoretical errors.

The $K^\pi=1^+$ collective band is also predicted by the *sd*-IBM2 as a neutron-proton asymmetric state. One cannot tell which model is suitable at present without relying on a microscopic calculation. If the difference between the d- and g-boson g factors turns out to be small, the *sdg*-IBM predicts weak $B(M1)$'s. The $B(M1)$'s in the low-lying states should be also calculated in the framework of the *sd*-IBM2. The results should be compared with the experiment.

C. Electric hexadecapole transitions

In the *sd*-IBM the $E4$ transition operator is expressed uniquely as $(d^\dagger\tilde{d})^{(4)}$, which is an SU(3) tensor (22). With this operator the $K^\pi=4^+$ band cannot be excited from

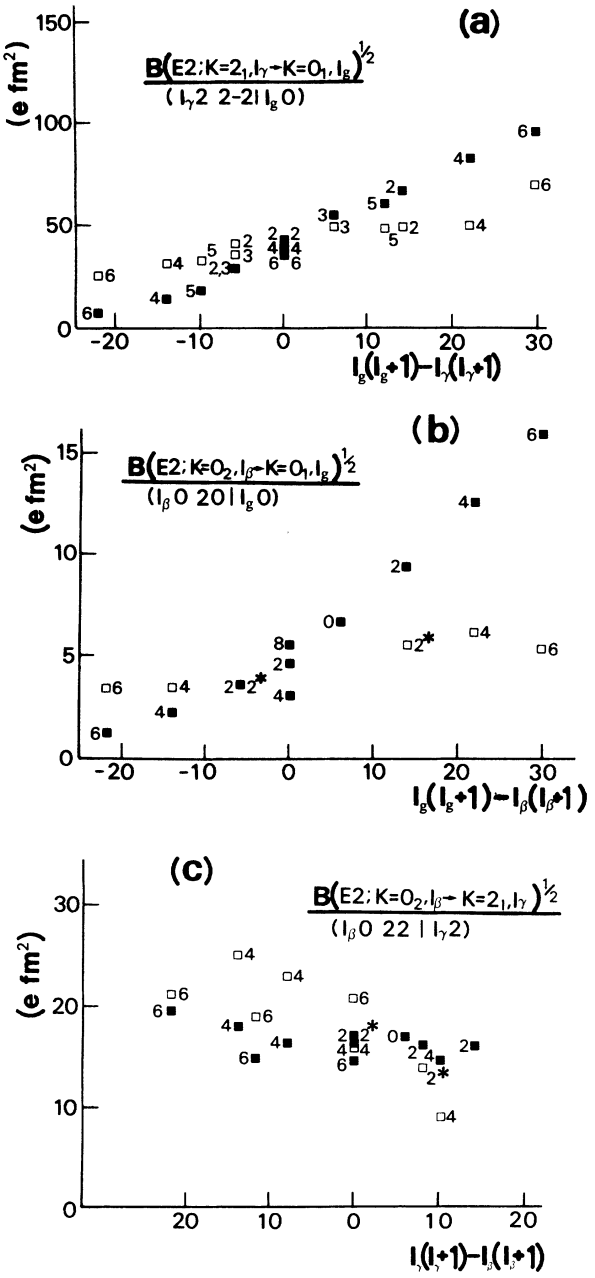

FIG. 10. (a) Mikhailov plot analysis of $E2$ matrix elements for the γ to the g transitions. Experimental values are shown by open squares while theoretical ones are shown by solid squares. Points are labeled by I_f. (b) Mikhailov plot analysis of the same elements for the β to the g transitions. Asterisks indicate that for the $I=2_\beta$ states only relative intensities have been determined. See Ref. 3 for more detail. (c) Mikhailov plot analysis of the same elements for the β to the γ transitions.

the ground state because of the SU(3) selection rule in the pure SU(3) limit. The experimental ratio is $B(E4;0_g^+\rightarrow 4_\gamma^+)/B(E4;0_g^+\rightarrow 4_g^+)=4.2$, which seriously contradicts the theoretical prediction 0.05 by the sd-IBM. Thus, it should be concluded that the sd-IBM is not able to reproduce the $E4$ excitations observed in ^{168}Er. By analyzing experimental data, Ichihara *et al.*[27] pointed out the importance of a hexadecapole degree of freedom in deformed nuclei. Nesterenko *et al.*[9] also introduced hexadecapole forces into quasiparticle-phonon-nuclear model (QPNM) for describing the $K_i^\pi=3_1^+$ band.

The hexadecapole degree of freedom is inherent in the sdg-IBM, and no extra freedom is needed. The one-body $E4$ operator is given by four independent parameters in this model:

$$T(E4)=e_1(s^\dagger\tilde{g}+\text{H.c.})+e_2(d^\dagger\tilde{d})^{(4)} +e_3((d^\dagger\tilde{g})^{(4)}+\text{H.c.})+e_4(g^\dagger\tilde{g})^{(4)} . \quad (4.9)$$

As in the $E2$ case, Eq. (4.9) can be transformed into a linear combination of four SU(3) tensor operators defined by Eq. (2.1). In terms of SU(3) tensor operators the sdg-IBM has (22), (33), and (44) tensor operators. Explicitly the $E4$ operator is written as

$$T(E4)=\sum_{K\lambda} a_{\lambda K} T_1^{\lambda,K,L=4} \quad (\lambda=2,3,4) . \quad (4.10)$$

For the $(\lambda,\mu)=(33)$ operator, K takes the values 1 and 3, but each operator is not Hermitian. A new Hermitian operator is given as follows:

$$\hat{T}^{\lambda=3}=\sqrt{5/82}\,T_1^{\lambda=3,K=1}+\sqrt{77/82}\,T_1^{\lambda=3,K=3} . \quad (4.11)$$

For (44), K takes 0, 2, and 4, we define new Hermitian operators as follows:

$$\hat{T}_A^{\lambda=4}=41\sqrt{3\times5/2\times7\times23\times383}\,T_1^{\lambda=4,K=0} +566\sqrt{2\times13/7\times23\times383\times683}\,T_1^{\lambda=4,K=2} +27\sqrt{3\times11\times13/2\times383\times683}\,T_1^{\lambda=4,K=4} ; \quad (4.12a)$$

$$\hat{T}_B^{\lambda=4}=-16\sqrt{3\times11\times13/3\times7\times23\times383}\,T_1^{\lambda=4,K=0} +319\sqrt{3\times5\times11/7\times23\times383\times683}\,T_1^{\lambda=4,K=2} +20\sqrt{3\times5/3\times383\times683}\,T_1^{\lambda=4,K=4} . \quad (4.12b)$$

The $E4$ operator is now rewritten by the newly determined four operators as

$$T(E4)=\alpha_1\hat{T}^{\lambda=2,L=4}+\alpha_2\hat{T}^{\lambda=3,L=4} +\alpha_3\hat{T}_A^{\lambda=4,L=4}+\alpha_4\hat{T}_B^{\lambda=4,L=4} . \quad (4.13)$$

The relations between parameters e's and α's are as follows:

$$\alpha_1=\frac{4}{\sqrt{5\times7}}e_1+\frac{19}{14\sqrt{7}}e_2-\frac{10\sqrt{11}}{7\sqrt{5\times7}}e_3+\frac{3\sqrt{11\times13}}{14\sqrt{5\times7}}e_4\ ,$$
$$\alpha_2=-\frac{44\sqrt{2}}{3\sqrt{3\times5\times7\times11}}e_1-\frac{22\sqrt{2}}{7\sqrt{3\times7\times11}}e_2$$
$$+\frac{\sqrt{2\times5}}{21\sqrt{3\times7}}e_3+\frac{12\sqrt{2\times13}}{7\sqrt{3\times5\times7}}e_4\ ,\qquad(4.14)$$
$$\alpha_3=\frac{\sqrt{2\times11\times13}}{\sqrt{383}}e_1+\frac{4\sqrt{2\times13}}{\sqrt{383}}e_3+\frac{4\sqrt{2}}{\sqrt{383}}e_4\ ,$$
$$\alpha_4=-\frac{148}{3\sqrt{3\times5\times383}}e_1+\frac{383}{14\sqrt{3\times383}}e_2$$
$$+\frac{2750}{21\sqrt{3\times5\times11\times383}}e_3+\frac{33\sqrt{13}}{14\sqrt{3\times5\times11\times383}}e_4\ .$$

The (3,3) operator excites the $K^\pi=1^+$ and 3^+ bands of the $(4N-6,3)$ representation from the 0^+ state of the $(4N,0)$ one. Similarly the $K^\pi=4^+$ bands belonging to $(4N-8,4)$ reps are excited through the (4,4) operators. In defining these two operators in Eq. (4.12), $\hat{T}^{\lambda=4}_B$ was constructed so that this operator does not excite the 4^+ states of $(4N-8,4)$ from the 0^+ state of $(4N,0)$. Neither the $w=0$ nor the $w=1$ member of the $K^\pi=4^+$ bands is excited by the $\hat{T}^{\lambda=4}_B$ operator. Thus, the *sdg*-IBM predicts a definite ratio for excitation amplitudes of the $w=0$ and $w=1$ states in the SU(3) limit. In the $N=16$ boson system this ratio is 1:6. Because of the two-phonon nature of the $w=0$ band[14] this band is only weakly excited. The observed relatively weak excitation of the $K^\pi=4^+$ band in ^{168}Er [$B(E4)=0.6$ spu] compared to that of the γ band[19] [$B(E4)=16.5$ spu] does not contradict its two-phonon nature. On the contrary, the QPNM prediction for the $K^\pi=4^+$ band is five times stronger than the experimental value.[9] Although a revised prediction of $B(E4)=0.8$ spu is reported by Soloviev,[28] the energy fit is worse and the $B(E4)$ for the γ band is three times smaller than the experimental value.

The three experimental $B(E4)$'s ($g\rightarrow g, g\rightarrow\gamma, g\rightarrow K^\pi=4^+$) in ^{168}Er can be used in a search for parameters in Eq. (4.13). One more datum is needed to fix four unknown parameters. Here it is assumed that the $g\rightarrow\beta$ $E4$ transition does not occur, because no member of the β band seems to be excited by the (α,α') experiment.[19] This point should be confirmed further by another experiment. The four parameters determined are $\alpha_1=1.106$, $\alpha_2=6.160$, $\alpha_3=5.001$, $\alpha_4=2.869$. The most striking prediction is the strong excitation of $K^\pi=3^+$ band. Its $B(E4)=50.8$ spu. Unfortunately we cannot currently compare this prediction with experiment, because the authors of Ref. 19 did not derive the experimental $B(E4)$ for this excitation. A coupled channel analysis of their experiment including the $K^\pi=3^+$ band would be very valuable for a test of the present model. The excitation of the $K^\pi_i=0^+_3$ band is predicted to be weak [$B(E4)=0.065$ spu]. Predictions are summarized in Table XII. In Table XIII diagonal $E4$ matrix elements of the g band are calculated. These values change remarkably as the angular momentum increases.

TABLE XII. The theoretical predictions of $B(E4)$ from the ground state to excited states and their experimental values in single particle unit.

Final band	Expt[a]	Theory	QPNM[b]	QPNM[c]
g	3.9	3.9[d]		
γ	16.5	16.5[d]		5.0
β		0.0[e]		
0^+_3		0.1		
3^+_1		50.8	0.8	
4^+_1	0.6	0.6[d]	3.3	0.8
2^+_2		18.9		
4^+_2		2.8		

[a]Reference 19.
[b]Reference 9.
[c]Reference 28.
[d]Fitted to experimental data.
[e]Assumed.

V. DISCUSSION AND CONCLUSIONS

One point which is not discussed in this analysis is the variation of the moment of inertia in each band. Bohr and Mottelson criticized the IBM on various points.[3] One criticism concerns the variation of the moment of inertia from one band to another. In this calculation we do not succeed in reproducing the L^2 and L^4 terms of excitation energies (See Table I of Ref. 3). The moment of inertia cannot be adjusted to experiment from band to band in a simple manner because in the present calculation it is fixed by the parameters chosen and the main part of the moment of inertia comes from the L^2 term of the Hamiltonian. Thus, the moment of inertia of the β band is predicted to be almost the same as that of the g band. On the other hand, experimentally the β band has a larger moment of inertia than the g band. It should be remembered that we have used only six parameters for the description of the energy levels. It might be possible to improve the calculated moments of inertia by introducing more parameters. This is still an open question.

In the present calculation the Hamiltonian is limited to include up to two-body interactions. This viewpoint is satisfactory if we successfully reproduce the overall experimental data. Indeed we have reproduced the overall data including the anharmonicity. It should be noted, however, that the anharmonicity problem is easily solved by introducing higher-order interactions, such as, three- or four-body interactions. This corresponds to the introduction of an anharmonic potential of γ. Actually,

TABLE XIII. Diagonal $E4$ matrix elements of members of the ground band in single-particle unit.

I^π	$\langle I\|\|T(E4)\|\|I\rangle$
2^+	-2.083
4^+	-1.311
6^+	0.279
8^+	3.640

Heyde and his collaborators[29] used cubic terms in the IBM in order to analyze ^{104}Ru.

Here we wish to show an example of a many-body interaction. If one defines an operator T by

$$T=[B^{\dagger}(42)\tilde{B}(24)]^{(00)} ,$$

then one finds the expectation value in the diagonal rep for the w quantum number ($\lambda+2\mu=4N$):

$$\langle T\rangle=\frac{\sqrt{5}}{420\sqrt{3}}\mu(4N-\mu+1)-\tfrac{5}{7}\sqrt{15}\langle S\rangle , \qquad (5.1)$$

where the operator S is defined by Eq. (2.8). For $w=0$ states $\langle S\rangle$ is equal to 0. In the large N limit $\langle T\rangle$ is proportional to μN in states with $w=0$. This means that T produces only a harmonic level scheme. The operator T^2 has an energy proportional to μ^2 as its leading term for those states. This apparently gives an anharmonic effect for the $K^{\pi}=4^+$ band. This example shows that one can very easily explain the anharmonic spectrum if one can introduce many-body interactions such as a T^2 operator.

Recently, Soloviev discussed the differences between his model and the *sd*-IBM.[30] His arguments may be divided into two parts as follows.

(1) The drawback of the IBM and of the Bohr and Mottelson model is the inclusion of a very small part of the space spanned by the two-quasiparticle states under consideration. These two models incorporate only β and γ degrees of freedom. Therefore these models can treat only states made by β,γ phonons, i.e., $\beta\beta,\beta\gamma,\gamma\gamma,\ldots$, phonons. He claimed that one must introduce such phonons as s', d', and g to describe excited states higher than the β and γ bands.

(2) According to his microscopic calculation the anharmonicity is so strong that no two-phonon states are predicted below 2.3 MeV. He claimed that the low-lying states below 2.3 MeV are not two-phonon states but one-phonon ones.

On the first point we partly agree with Soloviev. This is one of the reasons why we introduce the hexadecapole degree of freedom. Regarding the introduction of s' or d' bosons we do not have any microscopic reason to incorporate such degrees of freedom up to now as far as low-lying states are concerned.

The second criticism pinpoints the main difference between the Soloviev model and our model. His prediction differs not only from ours but also from the prediction made by Matsuo and Matsuyanagi.[31] They recently analyzed the same nucleus by using the self-consistent collective coordinate method.[32] They predicted that the two-γ phonon state lies around 2–2.4 MeV. Their model too, does not predict such a large anharmonicity as that of Soloviev.

One great difference between our model and Soloviev's model is seen in the prediction for the $E4$ transition strength from the ground state to the $I=4$ state of the $K^{\pi}=3^+$ band. In our model this band has high hexadecapole collectivity because of the explicit introduction of the hexadecapole degree of freedom. Thus, it is highly desirable to extract the $E4$ strength of this band experimentally because this state is indeed populated in the (α,α') experiment.[19]

In our model the $K_i^{\pi}=4_1^+$ state found experimentally is assumed to be a two-phonon state, whereas Soloviev predicts it as a one-phonon state. In the SU(3) limit we predict the $K_i^{\pi}=4_1^+$ bandhead state twice as high in excitation energy as the $K_i^{\pi}=2_1^+$ bandhead state. We have determined the parameters concerning the anharmonicity considering that the $K_i^{\pi}=4_1^+$ band starting at 2055 keV is a two-γ band. However, the 4^+ state at 2238 keV can be another candidate[22] as a member of a two-γ band. Higher-order interactions in the IBM would be really required when no two-phonon states are found experimentally below 2.5 MeV. Any experiment which reveals the nature of $K_i^{\pi}=4_1^+$ band is highly desirable.

In conclusion we have given a self-contained formalism of the *sdg*-IBM in the present paper. This model turns out to be very successful for a consistent description of energies and moments of ^{168}Er. In particular, since we have made predictions for $E4$ transitions using this model. The *sdg*-IBM seems to be a prominent theory for descriptions of deformed nuclei. At the same time the parameters of the phenomenological Hamiltonian must be calculated from the microscopic point of view. This is a problem for the future.

We would like to thank A. Gelberg for stimulating discussion. We also express our gratitude to D. M. Brink for reading the manuscript.

*Permanent address: Computer Centre, University of Tokyo, Tokyo 113, Japan.

[1]A. Bohr and B. R. Mottelson, Phys. Scr. **22**, 468 (1980).

[2]T. Otsuka, A. Arima, and N. Yoshinaga, Phys. Rev. Lett. **48**, 387 (1982); K. Sugawara-Tanabe and A. Arima, Phys. Lett. **110B**, 87 (1982); D. R. Bes, R. A. Broglia, E. Maglione, and A. Vitturi, *ibid.* **114B**, 86 (1982); N. Yoshinaga, A. Arima, and T. Otsuka, *ibid.* **143B**, 5 (1984).

[3]A. Bohr and B. R. Mottelson, Phys. Scr. **25**, 28 (1982).

[4]T. S. Dumitrescu and I. Hamamoto, Nucl. Phys. **A383**, 205 (1982).

[5]W. F. Davidson, D. D. Warner, R. F. Casten, K. Schreckenbach, H. G. Borner, J. Simic, M. Stojanovic, M. Bogdanovic, S. Koicki, W. Gellently, G. B. Orr, and M. L. Stelts, J. Phys. G **7**, 455 (1981).

[6]D. D. Warner, R. F. Casten, and W. F. Davidson, Phys. Rev. Lett. **45**, 1761 (1980); D. D. Warner, R. F. Casten, and W. F. Davidson, Phys. Rev. C **24**, 1713 (1981).

[7]N. Yoshinaga, Y. Akiyama and A. Arima, Phys. Rev. Lett. **56**, 1116 (1986).

[8]H. C. Wu, Phys. Lett. **110B**, (1982); H. C. Wu and X. Q. Zhou, Nucl. Phys. **A417**, 67 (1984).

[9]V. O. Nesterenko, V. G. Soloviev, A. V. Sushkov, and N. Yu. Shirikova, Dubna Report E4-85-856 and E4-85-878.

[10]V. K. B. Kota, Invited Talk at Work Shop on Interacting Boson-Boson and Boson-Fermion Systems, Gull Lake, Michigan 28-30 May 1984, edited by O. Schalten, p. 83 (unpublished).

[11]J. P. Draayer and Y. Akiyama, J. Math. Phys. **14**, 1904 (1973); J. P. Draayer and Y. Akiyama, Comput. Phys. Common. **5**, 405 (1973).
[12]Y. Akiyama, Nucl. Phys. **A433**, 369 (1985).
[13]K. T. Hecht, Nucl. Phys. **62**, 1 (1965).
[14]N. Yoshinaga, Nucl. Phys. **A456**, 21 (1982).
[15]Y. Akiyama, in *Proceedings of the International Symposium on Particle and Nuclear Physics, Beijing, China, 1985,* edited by Hu Ning and Wu Cheng-shi (World-Scientific, Singapore, 1986), p. 271.
[16]D. G. Burke, W. F. Davidson, J. A. Cizewski, R. E. Brown, E. R. Flynn, and J. W. Sunier, Can. J. Phys. **63**, 1309 (1985).
[17]D. G. Burke, B. L. W. Maddock, and W. F. Davidson, Nucl. Phys. **A442**, 424 (1985).
[18]D. G. Burke, W. F. Davidson, J. A. Cizewski, R. E. Brown, and J. W. Sunier, Nucl. Phys. **A445**, 70 (1985).
[19]J. M. Govil, H. W. Fulbright, D. Cline, E. Wesolowski, B. Kotlinski, A. Backlin, and K. Gridnev, Phys. Rev. C **33**, 793 (1986).
[20]T. Ichihara, H. Sakaguchi, M. Nakamura, T. Noro, F. Ohtani, H. Sakamoto, H. Ogawa, M. Yosoi, M. Ieiri, N. Isshiki, and S. Kobayashi, Phys. Rev. C **29**, 1228 (1984).
[21]Y. Akiyama, K. Heyde, A. Arima, and N. Yoshinaga, Phys. Lett. **173B**, 1 (1986).
[22]W. F. Davidson, W. R. Dixon, and R. S. Storey, Can. J. Phys. **62**, 1538 (1984).
[23]L. M. Greenwood, Nucl. Data Sheets **11**, 385 (1974); J. M. Domingos, G. D. Symons, and A. C. Douglas, Nucl. Phys. **A180**, 600 (1972).
[24]F. Iachello, Nucl. Phys. **A358**, 89c (1981); A. E. L. Dieperink, Prog. Part. Nucl. Phys. **9**, 121 (1983).
[25]A. Richter, invited talk presented at the Niels Bohr Centennial Symposium in *Proceeding of the Niels Bohr Centennial Symposium on Nuclear Structure, Copenhagen, Denmark, 1985,* edited by R. A. Broglia, G. B. Hagemann, and B. Herskind (North-Holland, Amsterdam, 1985); D. Bohle, G. Kuchler, A. Richter, and W. Steffen, Phys. Lett. **148B**, 260 (1984).
[26]*Table of Isotopes,* 7th ed., edited by C. M. Lederer and V. S. Shirley (Wiley, New York, 1978).
[27]T. Ichihara, H. Sakaguchi, M. Nakamura, T. Noro, F. Ohtani, H. Sakamoto, H. Ogawa, M. Yosoi, M. Ieiri, N. Isshiki, Y. Takeuchi and S. Kobayashi, Phys. Lett. **149B**, 55 (1984).
[28]V. G. Soloviev, Dubna Report, E4-87-45, 1987.
[29]K. Heyde, P. V. Isacker, M. Waroquier, and J. Moreau, Phys. Rev. C **29**, 1430, 1984.
[30]V. G. Soloviev and N. Yu. Shirikova, Yad. Fiz. **36**, 1376 (1982) [Sov. J. Nucl. Phys. **36**, 799 (1982)]; V. G. Soloviev, Dubna Report E4-84-602(1984).
[31]M. Matsuo and K. Matsuyanagi, Prog. Theor. Phys. **74**, 1227 (1985).
[32]T. Marumori, T. Maskawa, F. Sakata, and A. Kuriyama, Prog. Theor. Phys. **64**, 1294 (1980).